Growth, Modification and study of Tungsten trioxide thin films with Graphene oxide

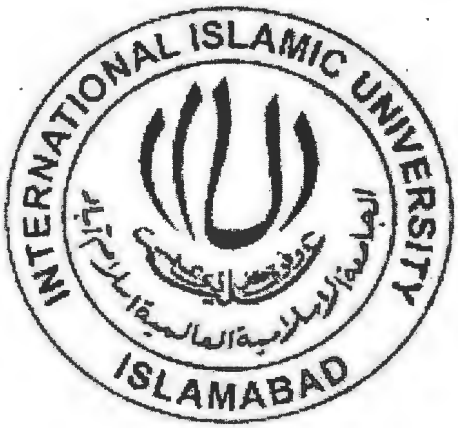

By

Aalia Saba

Reg. No. 333-FBAS/MSPHY/S15

DEPARTMENT OF PHYSICS

FACULTY OF BASIC AND APPLIED SCIENCES,

INTERNATIONAL ISLAMIC UNIVERSITY,

ISLAMABAD.

(2017)

Thin film

Nanocomposites

Tungsten Disulfide

Graphene oxide

X ray diffraction.

Growth, Modification and study of Tungsten trioxide thin films with Graphene oxide

By

Aalia Saba

(333-FBAS/MSPHY/S15)

Supervisor

Dr. Tariq Mahmood

Co-supervisor

Dr. Shamaila Sajjad

DEPARTMENT OF PHYSICS

FACULTY OF BASIC AND APPLIED SCIENCES,

INTERNATIONAL ISLAMIC UNIVERSITY,

ISLAMABAD.

(2017)

Starting with the name of Allah, the Most Gracious and the Most Merciful.

INTERNATIONAL ISLAMIC UNIVERSITY, ISLAMABAD.

FACULTY OF BASIC AND APPLIED SCIENCES,

DEPARTMENT OF PHYSICS.

Growth, Modification and study of Tungsten Trioxide thin films with Graphene oxide

By

Aalia Saba

(333-FBAS/MSPHY/S15)

A thesis submitted to

Department of Physics

for the award of the degree of

MS Physics

Signature: _____

Dr. Shamaila Sajjad
Chairperson
Department of Physics (FC, FBAS)
International Islamic University
Islamabad

(Chairman, Department of Physics)

Signature: _____

(Dean FBAS, IIU, Islamabad)

INTERNATIONAL ISLAMIC UNIVERSITY, ISLAMABAD

FACULTY OF BASIC AND APPLIED SCIENCES

DEPARTMENT OF PHYSICS

Dated: 20-06-2017

FINAL APPROVAL

It is certificd that the work presented in this thesis entitled "**Growth, Modification and study of Tungsten Trioxide thin films with Graphene oxide.**" by **Aalia Saba** bearing **Registration No. 333-FBAS/MSPHY/S15** is of sufficient standard in scope and quality for the award of degree of MS Physics from International Islamic University, Islamabad.

COMMITTEE

External Examiner

Dr. Parvez Akhter

Ex Director General Pakistan

Council of Renewable Energy Technology,

Islamabad

Internal Examiner

Dr. Waqar Adil Syed

Associate Professor

International Islamic University

Islamabad

Supervisor

Dr. Tariq Mahmood

Associate Professor

National centre for physics

Co-supervisor

Dr. Shamaila Sajjad

Assistant Professor,

Chairperson, Department of Physics

Department of Physics, FBAS, IIUI

Dr. Shamaila Sajjad
Chairperson
Department of Physics (FC, FBAS)
International Islamic University
Islamabad

A thesis submitted to

Department of Physics

International Islamic University Islamabad

as a partial fulfilment for the award of the degree of

MS in Physics

Declaration

I hereby declare that this thesis work, neither as a whole nor a part of it has been copied out from any source. Further, work presented in this dissertation has not been submitted in support of any application for any other degree or qualification to any other university or institute and is considerable under the plagiarism rules of Higher Education Commission (HEC), Pakistan.

Signature: ----------

Name: Aalia Saba

Reg. No. 333-FBAS/MSPHY/S15

Dedicated to my dearest parents for their love and support, sisters and my Niece Masfa.

Acknowledgement:

It gives me great pleasure and satisfaction to acknowledge the endowment of the creator of the universe, Allah Almighty, the most gracious, compassionate and beneficent to his creature which enabled me to complete my work successfully. I offered my humblest and sincere words of thanks to his Holly Prophet Mohammad (P.B.U.H) who is forever a source of guidance and knowledge for humanity.

I am thankful to my supervisor Dr. Tariq Mahmood, associate professor, national centre for physics, Islamabad for full cooperation and encouragement.

I feel great honour to express the deepest sense of appreciation to my respected co-supervisor Dr.Shamaila Sajjad, assistant professor, department of physics, IIUI, for her inspiring guidance, skilful suggestions and keen interest during the whole period of my studies. Her encouragement and unforgettable attitude have provided me a lot of opportunities to build my confidence in experimental work.

Special thanks to my best friend Madecha Jamshaid for helping me a lot in my hard times and giving me guidance where I needed. I shall express my heartiest thanks to Sanaia Shaheen and Anam Iqbal for being very supportive and co-operative throughout my research work.

I especially want to acknowledge efforts and prayers of my parents and sisters for their love, care and support in my life, which has been directly encouraging me for my study. My parent's prayers are always a source of my success. Allah may bless my parents and family with long life, health and happiness.

Table of Contents

List of Figures

List of tables:

List of Abbreviations

GO	Graphene Oxide
RGO	Reduced Graphene Oxide
WO_3	Tungsten Trioxide
XRD	X-Ray Diffraction
EDX	Energy Dispersive X-Ray Spectroscopy
SEM	Scanning Electron Microscope
FT-IR	Fourier Transform Infrared Spectroscopy
UV-Vis	Ultraviolet-visible Spectroscopy

Abstract

Hydrothermal method and modified hummer's method were used for the synthesis of Tungsten trioxide (WO_3) thin films and graphene oxide nanosheets respectively. Surface of Tungsten trioxide (WO_3) thin film is then modified with graphene oxide through spin coating method. After synthesis, the prepared samples were characterized by using different techniques XRD, SEM, EDX, and UV-Visible. XRD results indicated that the pure WO_3 thin films were in tetragonal (α-WO_3) and monoclinic (γ-WO_3) phases and after modification the prominent peaks of WO_3 were suppressed just because by introducing the contents of GO. The SEM results of the WO_3 thin films clearly showed the Nano brick like morphology and modified WO_3 nano bricks are wrapped by GO sheets and and it is feasible to differentiate the edges of single nano brick. UV-vis spectroscopy showed that maximum absorption of pure WO_3 is found at a wavelength of 523 nm while for modified WO_3 with GO Maximum absorption is found at 498 nm. The additional broad absorption was exhibited by modified WO_3 thin films in the visible region which lies in the range of 700-800. This absorption is due to O^{2-}–W^{6+} charge transfer transition, as in case of monoclinic WO_3.

CHAPTER NO. 1

1 Introduction

1.1 Thin Film:

Thin film is a material of fine microscopically thin layer of material that is deposited by several methods on to a glass or metal substrate. Thickness of thin film may vary from fraction of a nanometre to several micrometres. Different deposition parameters like temperature of source, film thickness, temperature of substrate, and deposition method can change the behaviour of a thin film [1].

Poortmans and Arkhipov have defined thin film as the film deposited by nucleation and growth process of invidually condensing molecules and ions on the substrate. They realized that the chemical, structural, and physical properties of thin films were strongly dependent on the thickness of the flims and deposition parameters. As indicated by them thin films may have variable thickness range from nanometer scale to few number of micro meter scales [2].

Cachet et al. stated that thin film with one dimension ought be so small such as the surface to volume ratio increases. They realized that the confined dimension of the film influenced the properties of the film. They well-defined the thin film as the two dimensional solid material. They stated that if the properties of surface and near surface were different from the properties of the bulk material then the thin films distinguished from the thick films [3].

Baran expressed that the rapidly changed thin film devices and materials have made the prospects for the development of new material, procedures and innovations. He clarified the significance and need of the fundamental resesarch activities for the increased knowledge and to build up the prescient capabilities for the chemical and physical properties of microstructures and thin films into different potential application [4].

1.1.1 Thin film and its nature:

Arbitrarily a thin film may be defined as a solid thin layer having thickness ranging from few angstroms to about 10μm or so. Meanwhile the thickness limitation is slightly arbitrary, somewhat thicker film may also come in the scope of the above definition. Therefore, the thickness of thin film is divided into the following categories;

i. Ultra-thin film which ranges from few to about 50-100Å.

ii. Thin (or very thin) ranging from 100-1000Å.

iii. Comparatively thicker one generally being greater than 1000Å.

It is demonstrated that the above confusion in understanding the definition of the film thickness is further complex by coinage of new term, i.e. thick film which is of extremely pragmatic significance. This new term specifies totally new class of film instead of the composite layer film. Thickness of these films is about 10μm and even often more than this.

Usually, there are no limitations on the dimensions under which a material might be called as a thin film. Any two-dimensional materials which works differently in contrast to its bulk material and has high surface to volume ratio falls in to thin film class. Distinctive behaviours are because of the reduction of material in one dimension to few atomic layers thus the two surfaces come so close to each other that they effect the physical properties of a material that are not present in its bulk counterpart. But in literature, the thin film dimensions are within few nanometre to a few micrometre [5].

1.1.2 Thin film versus powder:

As one dimension of the thin film ought to be so small to such an extent that it effects the properties of thin films. Hence, the optical, structural, and electrical properties changes because of confine dimension of thin film. Therefore, the material exhibit tuneable properties because of confinement dimension. This effect is called quantum confinement and depends on the thickness of thin film [6].

Thin films found not quite same as bulk materials because thin films were not fully dense and had two dimensions with the third confined dimension. Thin films were influenced by the interface effects and deposited with variation of the materials. Thin film coatings were found independently with the thermodynamic compositional constraints [7].

1.1.3 Factors affecting the growth, structure and film properties:

There are various factors that affect the growth, structure and properties of a deposited film. These are;

- Substrate temperature
- Source temperature
- Nature of the substrate
- Contamination by impurities and presence of defects on the substrate surface
- Annealing

Two significant parameters film thickness and temperature of substrate affect the properties of film. Throughout the process of deposition, the mobility of the deposited atoms on the surface of substrate can be enhanced by increasing temperature of substrates.

1.1.4 Applications of thin films:

Several applications of thin films used for the progress of solid state electronic devices and integrated circuits in micro-electronics. In electronic displays, such as light emitting diodes, liquid crystal displays, plasma, electro-chromic and florescent displays thin films of conductive transparent material were being used commonly. In the field of optical coatings, thin films of anti-reflecting film coatings were used as interference filters for solar panels and as infrared solar reflectors. Thin magnetic films and optical coatings were used for data storage devices in computer memories and compact disks. Thin films of carbide, nitride and borides were used as hard coatings to enhance the wear resistance of metal surfaces for tools and machine parts. Diamond like carbon films were also used for hard surface coatings. Thin films were found very useful in different decoration pieces, such as wrist watches, eye glass frames and in other decorative parts [8]. Detail of some application is given below.

- **Decorative coatings:**

For decorative coatings, the use of thin films probably signifies their oldest application. Today, thin film materials of high refractive index and variable thickness e.g titanium dioxide are frequently functional for attractive coatings on glass e.g., creating a rainbow-colour appearance as oil on water. Also, by sputtering of gold or titanium nitride transparent gold-coloured surfaces may either be prepared.

- **Optical coatings:**

These layers assist in both refractive and reflective systems. Larger-area reflective mirrors which were available during 19th century and were formed on glass by sputtering of metallic aluminium or silver. Refractive lenses in optical instruments e.g. in microscopes and cameras commonly show aberrations. These lenses show non-ideal refractive behaviour. Whereas along the optical path large sets of lenses must be lined up earlier, currently, these aberrations' may correct with the coating of optical lenses by transparent multilayers of silicon nitride, silicon oxide or titanium dioxide etc. A notable case for the development in optical frameworks by thin film technology is signified by a limited mm wide lens used in smart phone cameras. Further examples are assumed by anti-reflection coatings on solar panels or eyeglasses.

- **Protective coatings:**

Thin films are frequently fabricated to defend a fundamental work piece from external influences. The protection can work by lessening the interaction with the exterior medium so as to decrease the diffusion to work piece from medium. Frequently, between mechanically moving parts thin films assist as protection against abrasion.

- **Thin-film photovoltaic cells:**

Thin-film advancements are progressed by means of considerably lessening the cost of solar cells. Thin film solar cells are inexpensive to manufacture due to their reduced material costs. This is particularly signified in usage of printed electronics procedures.

- **Thin-film batteries:**

To create unique batteries for particular applications thin-film printing expertise is utilized to apply solid-state lithium polymers to a variation of substrates . Thin-film batteries can be deposited directly onto chip packages in any size or shape [9].

1.2 Tungsten Trioxide:

When contrasted with other metal oxide efficient nanostructure, as ZnO, NiO, TiO_2 several other, considerable progressive studies on chromic properties of WO_3 has been made. WO_3 is a well considered material in application like dye sensitized solar cells, sensing and photocatalysis [10].

Because of extremely exceptional physical and chemical properties of WO_3, it has accomplished great scientific concentration. Associated with other materials, WO_3 has stable physicochemical properties, deeper valence band (+3.1 eV), strong photo corrosion stability in acqueous solution, small band gap energy (2.4-2.8 eV), and very stable recylability performance. It has the refractive index of 1.

Between a variation in tungsten oxides, just four of them are of incredible significance. They all have attractive colours, (dark blue), WO_2 (chocolate brown), WO_3 (yellow), , and $W_{18}O_{49}$ have the violet colour. Structurally So-called higher tungsten oxides are correlated to both the $W_{20}O_{58}$ and WO_3 structures.

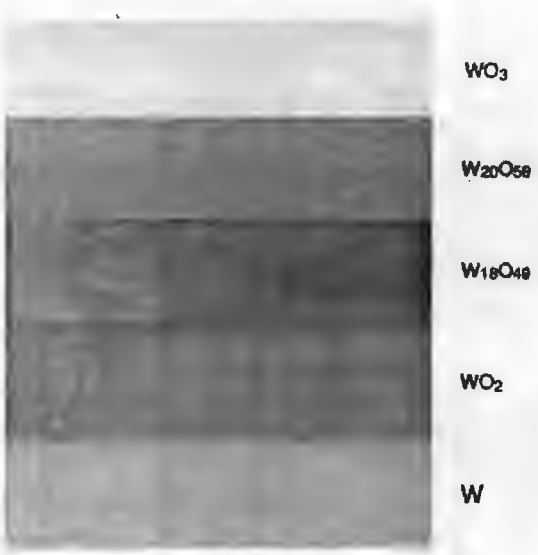

Figure 1.1: Different colours of tungsten oxides

They show colours from yellow to green to very dark. The colour variation is due to a slight loss of oxygen which introduces a new valence state in the structure of WO_3, either W^{5+} or W^{4+}. Cation to cation charge transfer among the parent W^{6+} and a reduced ion is the reason for the change in colour [11].

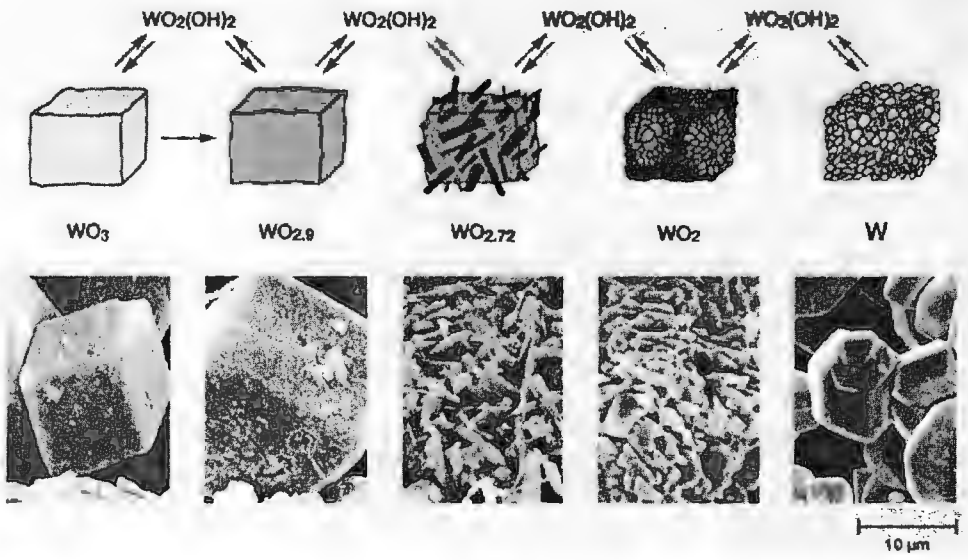

Figure 1.2: step by step production of tungsten oxides and tungsten metal from WO_3

1.2.1 Structural information of tungsten oxides:

WO_3 crystals have ABO_3 perovskite like structure and are usually constructed by sharing the corners and edges of WO_6 octahedral [12]. Tungsten trioxide's structure depends on

temperature. At least five phase transitions are shown by Pure WO_3 crystals from −180 to 900 °C

Table 1: Phase transition of pure WO3 crystals

WO_3 crystals structures	Temperature
Tetragonal (α-WO_3)	> 740 °C
Orthorhombic (β-WO_3)	330–740 °C
Monoclinic I (γ- WO_3)	17–330 °C
Triclinic (δ-WO_3)	−43–17 °C
Monoclinic II (ε-WO_3)	< −43 °C

Between the five crystal forms, at room temperature, γ-WO_3 is the most stable phase in bulk WO_3. Therefore, "WO_3" commonly refers to γ-WO3. A comparatively stable crystal structure is hexagonal (h-WO_3), but when annealed at temperatures above 400 °C it will change into γ-WO_3 [13]. For nanostructureWO_3, phase transition temperature is commonly lower as compared to bulk WO_3 [14]. At room temperature, in some nanostructured WO_3 the orthorhombic crystal phase can be retained [12]. Further, α-WO_3, is stable only above 725 °C, can also be retained using a low cooling rate[15].

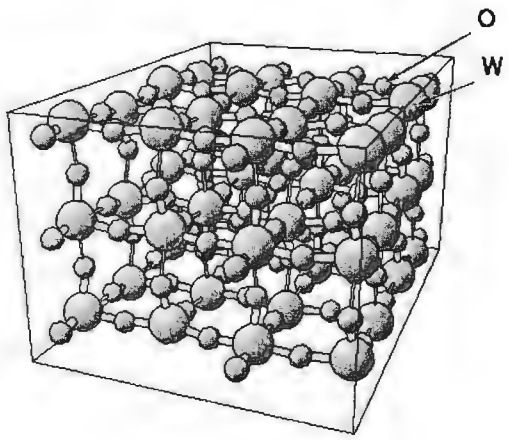

Figure 1.3: Lattice structure of WO_3

1.2.2 Properties of Tungsten trioxide:

Tungsten oxide (WO_3) is an n-type indirect semiconductor with a band gap of 2.5–3.2 cV[16-18] and comparatively high conductivity, which has many exciting optical, electrical and structural properties.

Table 2:Properties of Tungsten trioxide

Properties	
Chemical formula	WO_3
Molar mass	231.84 g/mol
Appearance	Canary yellow powder
Density	7.16 g/cm^3
Melting point	1,473 °C (2,683 °F; 1,746 K)
Boiling point	1,700 °C(3,090 °F;1,970 K) approximation
Solubility in water	Insoluble
Solubility	slightly soluble in Hydrofluoric acid

1.2.3 Applications:

Because of the adaptable nature of WO_3 nanoparticles, they have been broadly utilized as a part of different fields. Due to flexibility of tungsten oxide it is utilized for various applications. The applications of WO_3 are found in sensors, devices, catalysts, and miscellaneous applications. As shown in Figure 1.4 these applications could be more characterized by use.

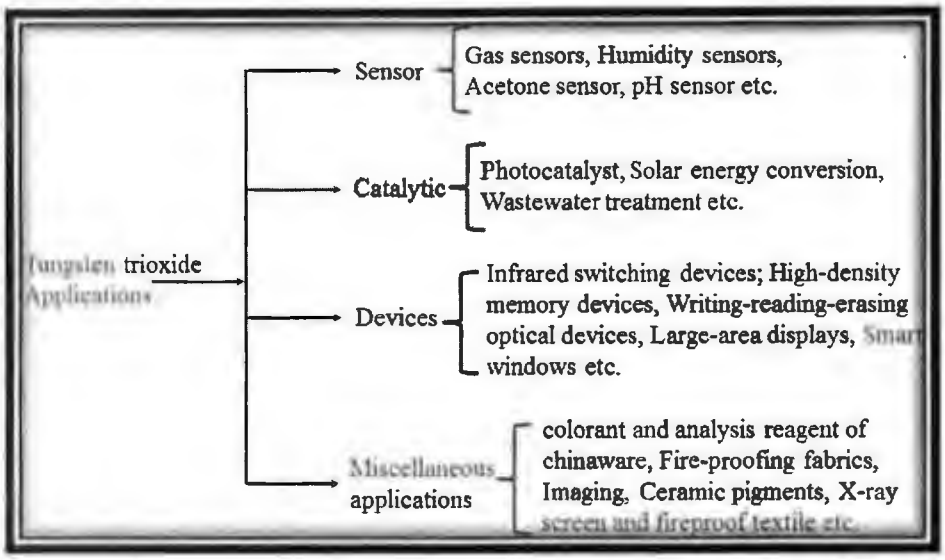

Figure 1.4: applications of tungsten trioxide

➢ Sensors:

For the application of gas sensing various kinds of semiconducting metal oxides are famous like TiO_2, SnO_2, CuO, In_2O_3, Fe_2O_3, CdO, ZnO, TeO_2, MoO_3 and WO_3. Diverse metal oxides indicate distinctive gas sensing properties as a result of their stoichiometry-dependent conductivity and in addition their interstitial anion and cation vacancies [19]. The principle of gas sensors is based on the adsorption of gases on the surface due to which the electrical resistance of the sensor changes. Tungsten oxide is an n-type semiconductor and is valid for reducing and oxidizing gas species [20]. As there are many applications of tungsten trioxide, but is most commonly used in the field of sensors.

➢ Catalysis:

WO_3 have been utilized in numerous catalytic applications like solar energy conversion or photocatalysis, and waste water treatment. Due to wide band gap energy tungsten trioxide is very familiar and it can absorb over a long range of visible light, bestowing it among several applications in the field of photo catalysis.

➢ Devices:

Another significant application of tungsten trioxide is devices. WO_3 could be benefitted in several devices, such as high-density memory devices, infrared switching devices, large-area displays, smart windows and writing-reading-erasing optical instruments. For these types of applications, material's electrochromic properties are responsible, allowing it to alter optical

properties reversibly and continuously with a small electric difference. WO_3 in combination among various materials and with different morphologies shows enhanced electrochromic properties.

➢ Miscellaneous applications:

Furthermore, WO_3 could be utilized as an analytical reagent and colorant in fire-proofing fabrics, X-ray screens, ceramic pigments and fireproof textiles. WO_3 is used in paints and ceramics as a pigment due to its rich yellow colour [21]. The composite structure of tungsten trioxide is also beneficial in several new applications.

Somewhere else the above applications, WO3 can likewise be used as a systematic reagent and colorant for chinaware and in insulating textures, X-beam screens, clay shades and flame resistant materials. WO3 is utilized as a part of paints and earthenware production as a shade because of its rich yellow shading [21]. The composite structure of tungsten trioxide is additionally gainful in a few new applications.

1.3 Graphene Oxide:

Graphene oxide can also be termed as graphitic acid or graphite oxide is a 1nm thick compound in variable ratios of carbon, oxygen, and hydrogen. It contains carboxyl, hydroxyl, ketone, ep-oxide and ester functional groups attached with carbon atoms.

GO is a monolayer nanomaterial of graphite oxide and can be attained into layered sheets by exfoliating graphite oxide through mechanical stirring or sonicating [22]. The graphene-based lattice and presence of numerous oxygen-containing groups primarily hydroxyl and epoxy and groups permit GO abundant enthralling properties. First, the functional groups present on graphene oxide surface act as operative anchoring sites to immobilize numerous active species. Moreover, electronic properties of GO are tuneable. In sp3 hybridization, a large portion of carbon atoms is bonded with oxygen atoms, due to which GO is characteristically insulating having sheet resistance of 10^{12} Ω sq^{1} or higher. But the sheet resistance decreases after reduction to RGO. Thus, the material becomes a semiconductor or a graphene-like semi-metal. It has been revealed that by controlling coverage, relative ratio and assembly of the hydroxyl and epoxy groups, band gap of GO can be tailored [23, 24].

In addition, GO also shows outstanding mechanical and optical properties for an extensive landscape of applications. The optical transmittance of GO films can be continuously modified by changing the thickness of films or the level of reduction [25].

1.3.1 Structural features:

Analogous to synthetic methods, the precise structure of GO has also significantly changed over time, and even to this day no definite model be present. There are several reasons for this, but the main contributors are the nonstoichiometric atomic composition, complication of the material with sample-to-sample variability due to its amorphous structure, and the non-existence of accurate analytical techniques meant for characterizing such materials. Despite these difficulties, substantial effort has been focused toward understanding the structure of graphene oxide, considerable of it with great success.

1.3.1.1 Initial Models:

In 1939, Hoffman & Holst proposed the first structure of graphene oxide. According to this model, it was supposed that on sp^2 graphitical basal plane, only carbon atoms were covalently bonded to epoxy groups and the molecular formula was estimated to be C_2O [26]. In 1946, Ruess planned the first model to introduce graphene oxide as a hybrid sp^2/sp^3 network, as opposed to only a sp^2 network like graphite. Additionally, he represented the hydrogens by recommending that hydroxyl groups were covalently bonded to the graphitic basal plane in accumulation to epoxides [27]. In the Reuss model an obvious misconception was that it presumed a lattice structure with a definitive repeat unit[3] which directed to several different structures to expand on this thought, but with slight distinctions in the chemical composition. In 1969, Scholz and Boehm proposed a model that entirely detached the epoxide and ether groups, replacing regular quinoidal species in a grooved backbone [28].

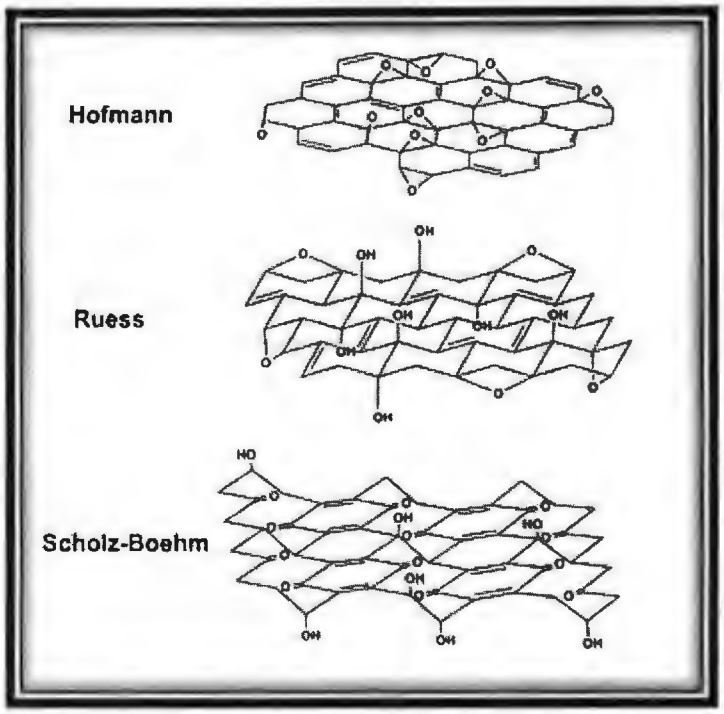

Figure 1.5: The structural evolution of GO over the years.

On the inhomogeneity of graphene oxide nothing of these structures focused, though, The Lerf-Klinowski model, which was proposed in 1998, was the first to do as such.

1.3.1.2 Lerf-Klinowski Model:

For graphene oxide, the most familiar and broadly accepted structural model is the Lerf- Klinowski. Lerf and coworkers done initial studies through cautious analysis of solid-state nuclear magnetic resonance spectra on the way to characterize the material. This was a first for the field as previous models relied mainly on reactivity, elemental composition and X-ray diffraction studies. In revolutionary work of Klinowsky and Lerf they suggest that graphene oxide is made up of non-oxidized aromatic patches of inconstant size and these patches are detached from each other by aliphatic six membered rings comprising epoxide groups, double bonds and hydroxyl groups. In Lerf-Klinowski model, the Oxygen functional groups lie below and above both, the basal plane, giving rise to the hydrophilic behaviour and polar nature of graphene oxide.

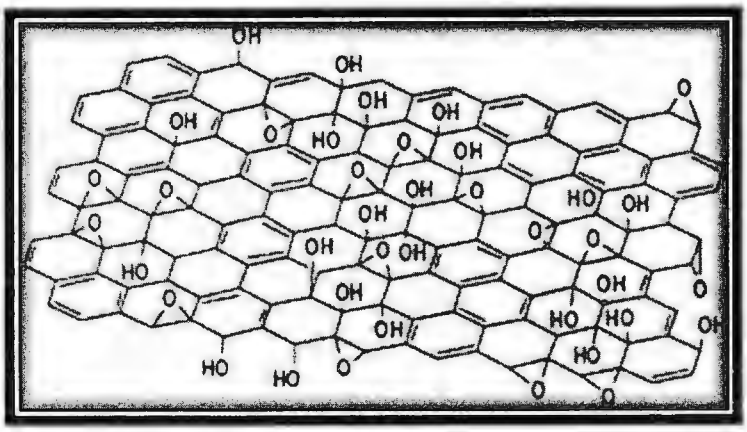

Figure 1.6: Chemical structure of graphene oxide based on the Lerf–Klinowski model.

1.3.2 Synthesis of Graphene Oxide:

Graphene Oxide can be obtained through natural graphite by three different methods:

1.3.2.1 Broide's Synthesis:

In 1859, a British chemist B.C. Brodie was examining the reactivity of flake graphite and investigated the structure of graphite [29].This endeavor of Brodie leaded to the formation of graphene oxide. Brodie performed one reaction in which he used the mixture of potassium chlorate ($KClO_3$) and fuming nitric(HNO_3) acid with graphite and he noticed that after heating the dull grey graphite had put on weight and gone up against a light yellow color [30]. Brodie revealed that the resultant material was composed of carbon, oxygen and hydrogen, resultant in an increase in the total mass of the flake graphite. Brodie, upon weighing the substance, also observed that the substance had got weight from the original graphite used that was a sign of oxidization.

1.3.2.2 Staudenmaier's Synthesis:

In 1898 by L. Staudenmaier improved Broide's work to a next step, in which he introduced two main variations in Broide's method.

- To increase the acidity of the mixture he added concentrated sulfuric acid.
- Into the reaction mixture solution added various aliquots of potassium chlorate completed the course of reaction.

These variations lead to an extremely oxidized product yet the product composition was similar as that of Boride's.

This reaction was a continuous risk to explosion also exceptionally time consuming that is the reason this process was not worth performing.

1.3.2.3 Hummer's Synthesis:

Almost 60 years afterward Staudenmaier experimentation, an alternate oxidation method was developed by Hummers and Offeman for synthesis of graphene oxide. They reacting graphite with a mixture of concentrated sulfuric acid (H_2SO_4) and potassium permanganate ($KMnO_4$) again, attaining similar levels of oxidation [30].

These three methods include the key routes for forming GO. Significantly, it has since been exhibited that the results of these reactions show strong variance, depending on the specific oxidants used, as well as on the reaction conditions and graphite source.

1.4 GO based nanocomposites:

Graphene is chemically inert so, in aqueous and nonaqueous solvents it has poor dispersibility and it cannot interact with other polymer elements. However, the Graphene oxide has been generally utilized for all functional composites due to its its oxygenated functional groups that make growth of numerous inorganic nanostructures more appropriate. When graphene oxide is combined with other organic or inorganic components, it can prompt new changes in mechanical properties, thermal conductivity and electrical conductivity of other polymer based materials. Therefore inorganic nanostructure composites are too generally prepared with graphene oxide that have potential applications in optics, photo catalysis, optoelectronics, bio/sensing, fuel cells, supercapacitors and batteries.

By utilizing numerous fabrication methods, a huge numbers of inorganic nanostructures have been integrated with GO or RGO that comprises like WO_3, Fe_2O_3, ZnO, TiO_2, MnO_2, Co_3O_4 $W_{18}O_{49}$, and Fe_3O_4, hydroxides like FeOOH and $Ni(OH)_2$, metals like Pt, Au and Ag.

Aims and Objectives of the Work:

This MS work has specific objectives which are described as follows and their detail is described in the next chapters.

- To synthesize tungsten trioxide thin films by hydrothermal method.
- To synthesize Graphene Oxide by modified Hummers method.
- To modify tungsten trioxide thin films with graphene oxide through spin coating.
- The prepared samples were characterized thoroughly with different characterization techniques such as X-ray diffraction (XRD), scanning electron microscopy (SEM), UV-Visible.
- Compared the pure WO_3 thin films with modified WO_3 thin films with GO in above mentioned characteristics.

CHAPTER NO. 2

2 Literature review

Zhihui Jiao et al, deposited Tungsten trioxide hydrate ($3WO_3.H_2O$) films directly on fluorine doped tin oxide (FTO) substrate with different morphologies by hydrothermal method. Scanning electron microscopy(SEM) analysis reveals that $3WO_3.H_2O$ thin films composed of wedge like, sheet like and plate like, nanostructures could be selectively synthesized by adding $(NH_4)_2SO_4$, CH_3COONH_4 and Na_2SO_4 as capping agents, respectively. X-ray diffraction(XRD) studies showed that the structure of these films were orthorhombic. After dehydration prepared thin films showed noticeable photocatalytic activities [31] .

Kai Huang et al, synthesized hexagonal WO_3 (h-WO_3) nanorods successfully by hydrothermal method using Na_2SO_4 as a precursor. Uniform nanorods with lengths of up to several micrometres and diameters of 100–200nm are obtained. With different quantities of Na_2SO_4 the growth mechanism and morphology were examined. Experimental parameters could lead to different morphologies and structures of the concluding products in this experimentation. The present perceptive of the growing procedure of the above-mentioned nanostructures theoretically gives significant data about the morphology and structure of tungsten trioxide and further oxides. They also examined Prepared hexagonal WO_3 nanowires as anode materials of Li-ion batteries for electrochemical performances. The outcomes infer that for Li-ion batteries, hexagonal WO_3 nanorods are favourable anode materials [32].

Samuel Hong Shen Chan and co-workers reported that tungsten trioxide, WO_3 is very effective and active photo catalytic material for degradation of dyes in waste water. Curz et al defined that various morphologies and physical properties are responsible for treatment effectiveness such as band gap energy and surface area. Moreover, they do not find tungstate a multipurpose photo catalyst when compared to TiO_2, but for some particular dyes it is still proved to be useful catalyst [33].

Yuanmeng et al. used electro chemical method to prepared WO_3-graphene composite, with a one-step treatment assisted with twelve tungsten phosphate acid. Nanoparticles of WO_3 were spread on GO sheets and allowed to absorb light and transfer electrons. Electron-hole pair recombination was blocked as graphene plate role of electron acceptor material. Due to the properties of single crystalline WO_3 Nano rods it is easier for electrons to move between graphene sheets and WO_3, which is responsible for more reactive sites on surface of WO_3 and GO sheets in degrading dyes. Therefore, nanocomposites of WO_3/GO exhibit higher

photocatalytic activity than pure WO_3 Nano rods under the UV light irradiation. The UV results revealed 2.2 times enhanced photocatalytic activity of WO_3/GO sheets than by GO and WO_3 [34].

Penza et al. considered the NO_x gas sensing features of tungsten trioxide thin films which are activated by noble metals (Pt, Au, Pd,) layers and informed that at low temperature the activator layers had a positive effect on the speed of response to NOx and on selectivity enhanced with respect to other reducing gases (SO_2, NH_3, CO, H_2, CH_4, H_2S,) [35].

Nengjie Huo et al, synthesized tungsten oxide (WO_3) nanostructures like nanotubes bundles, nanowires and nanorods bundles by hydrothermal method. For the first time the ultraviolet (UV) photo response characteristics of the devices containing these WO_3 nanostructures are investigated. They found that hexagonal-WO_3 nanowires showed very excellent UV photo response property. They report that h-WO_3 nanowires with fewer defects and large specific surface area exhibit very excellent UV photo response property through switch ratio (defined as I_{photo}/I_{dark}) as high as 60 [36].

M. Acosta et al, synthesized tungsten oxide thin films substrates by using RF Sputtering on glass at room temperature utilizing tungsten trioxide target for numerous values of the argon pressure (P_{Ar}). The morphological and structural properties were studied by means of atomic force microscopy and X-ray diffraction. Films were crystallized in a mixture of monoclinic and hexagonal phases were obtained after annealing at 350 °C. After thermal treatment, roughness of surface was enlarged by an order of magnitude 1 nm to 20 nm. However, on the optical properties of films, the argon pressure showed a strong impact. Furthermore, the study of optical properties specified three regions as light blue films for 2.67 Pa $<P_{Ar} < 6$ with intermediate transmittance values, deep blue films for $P_{Ar} \leq 2.67$ Pa with low transmittance values and transparent films for $P_{Ar} \geq 6$ Pa with high transmittance values. They propose that optical properties changes when the growth argon pressure decreases due to the increase in argon vacancies numbers [37].

Wang, Z-g et al, [38] determined the green synthesis of reduced graphene oxide (RGO) and its electrical properties. Graphene oxide (GO) was synthesized by modified Hummer's method. Reduction of graphene oxide was done by two different methods, ethanol-thermal reaction and hydrothermal reaction. Products were characterized by XRD, TEM and XPS. Results study reveals that ethanol is more effective reducing agent for reduction of GO than the supercritical water under solvothermal condition. Which causes that RGO reduced by ethanol has lower

oxygen contents but higher electrical conductivity than RGO synthesized by hydrothermal reaction.

Xiaoqin Jie et al, used a facile sol–gel method to synthesized Graphene (GR)-wrapped WO_3 Nano sphere composite. The GR-WO_3 nanocomposites were characterized by X-ray powder diffraction (XRD), field emission scanning electron microscopy (FESEM), Raman spectroscopy and transmission electron microscopy (TEM). These Nano spheres composite shows p-type gas sensing behaviour and the response of GR-WO_3 sensor regarding NO_2 exhibited that with an increase in the concentration from 7 to 56 ppm resulted in linear increase at room temperature[39].

Song, J., X. Wang et al, synthesized GO sheets from modified Hummer's method and by using transmission electron microscopy (TEM) they determined microscopic morphologies of GO sheets. To determine the optical properties of the graphene oxide sheets, UV-Vis spectroscopy was used by them. UV-Vis results revealed that in the visible range of 380~800 nm GO acquired good absorption, however slightly decreased absorption was observed in the ultraviolet range. Therefore, photo response of GO sheets was found in ultraviolet range as well as in visible range, which indicated the enormous potential used for application of light. They also investigated average crystalline properties of the GO sheets by XRD and results of XRD demonstrated the successful synthesis of GO sheet [40].

Xiaoqiang an et al, investigated the incorporation of WO_3 Nano rods and graphene nanocomposites used for NO_2 gas sensing and high-efficiency visible-light-driven photocatalysis. Nanostructures with one-dimension have enormous significance due to superior charge transport properties. This new composite shows strangely enhanced performance for these applications as compared to pure WO_3 nanorods. The efficient photocatalytic activity of nanocomposite of WO_3/graphene is related to the improved adsorption towards enhanced light absorption, efficient charge separation and chemical species[41].

M. Choobtashani et al, used thin films of tungsten oxide for photocatalytic reduction of graphene oxide platelets on surface of the films under UV or visible light of the environment. To characterize tungsten oxide films and graphene oxide sheets AFM (Atomic force microscopy) technique was used. Moreover, to investigate photocatalytic reduction of the graphene oxide platelets and chemical state of the tungsten oxide films X-ray photoelectron spectroscopy (XPS) is used. on surface of the sol–gel tungsten oxide film the reduction level of GO was attained after 24 hours UV-assisted photocatalytic reduction which was similar to

the reduction level generally obtained by hydrazine. The tungsten oxide film prepared by sol–gel exhibited an efficient photocatalytic reduction of the Graphene Oxide platelets after exposure for 2 days to the visible light[42].

Dreyer, D.R.et al. clarified that Staudenmaier and Brodie both used $KClO_3$ and nitric acid to synthesize graphene oxide. Nitric acid reacts strongly with carbon surfaces because it is a strong oxidizing agent. Oxidations by HNO_3 caused in the release of gaseous NO_2. Correspondingly, potassium chlorate ($KClO_3$) is a strong oxidizing agent generally used in explosive materials or in blasting caps. Therefore, their methods produced many side products and were highly hazardous. As an alternative of it, Hummers method utilized a combination of potassium permanganate and sulfuric acid [29].

Sakthivel Thangavel et al, synthesized nanocomposite of tungsten oxide and reduced graphene oxide WO_3/rGO. They also studied physical properties of these nanocomposites. By using a simple chemical method, the WO_3-rGO nanocomposite was prepared and the same was reduced by microwave irradiation. Characterization of these nanocomposite was done by XRD, SEM and AFM techniques. The X-Ray diffraction analysis showed the tetragonal phase of WO_3. By using UV-Vis and Photoluminescence (PL) spectroscopy the optical property was analyzed. By Raman spectroscopy layer defect in rGO was analysed. The PL results revealed that the emission peak for rGO and WO_3-rGO nanocomposite were found at 389 nm and 450 nm, respectively. By degradation of Methylene Orange dye at two different concentrations of WO_3-rGO (1 mg and 5 mg) the photocatalytic characteristic WO_3-rGO composite was analysed. Fourier Transform Infra-Red Spectroscopy identified the presence of functional groups. Results reveal the potential application of WO_3-rGO nanocomposite in photo catalysis [43].

E. Luevano-Hipolito et al, used precipitation method to prepared WO_3 polyhedral particles using PEG (polyethylene glycol) being as steric stabilizer and template. By the thermal treatment the aggregation degree and growth of WO_3 polyhedral particles were affected, which produced distinct physical properties. Samples were characterized by scanning electron microscopy (SEM), X-ray powder diffraction (XRD), adsorption–desorption N_2 isotherms (BET) and UV–vis diffuse reflectance spectroscopy (UV–vis DRS). WO_3 samples were tested as photo catalysts under UV irradiation in the oxidation reaction of nitric oxide (NO). The photocatalytic activity of the samples was related to their surface area values and its

morphology. For the application of air purification they demonstrated that by elimination of NO, polyhedral particles of WO_3 are active photocatalytic functional materials [44].

CHAPTER NO. 3

3 Experimental Methods

In the experimental procedure, I synthesized tungsten trioxide thin films by Hydrothermal growth method and graphene oxide nanosheets by Modified Hummers method. After synthesis, I modify the surface of the tungsten trioxide thin films by graphene oxide nanosheets.

3.1 Instrumentation:

Following instruments were used during the synthesis process.

- Beakers
- Magnetic stirrer
- Hot plate
- Centrifuge machine
- Furnace
- Sonication bath
- Drying Oven
- Weighing balance
- Autoclave
- Spin coater
- Teflon stand

3.2 Materials and Reagents:

Table 3: Materials and Reagents

CHEMICALS	FORMULAS
Sodium tungstate	Na_2WO_4
Hydrochloric acid	HCl
Deionized Water	H_2O
Sulphuric acid	H_2SO_4
Nitric Acid	HNO_3

Natural Graphite	C
Potassium Permanganate	$KMnO_4$
Hydrogen Peroxide	H_2O_2
Ethanol	CH_3-CH_2-OH

3.3 Different deposition techniques of Tungsten trioxide thin films:

To deposit WO_3 thin films, several techniques have been used. WO_3 thin films can be synthesized by

- electrospinning
- pulsed laser deposition
- chemical vapour deposition
- anode oxidation
- sol–gel
- thermal evaporation
- sputtering
- hydrothermal approach.

I followed the Hydrothermal deposition method to prepare the tungsten trioxide thin films.

3.4 Why Hydrothermal deposition method?

I attempt to design nanostructured WO_3 thin films by simple hydrothermal approach.

Because Hydrothermal approach is cost-effective, facile and dominant tool to control over the growth and size at low temperature [45, 46].

Hydrothermal Growth method employed for the growth of WO_3 on fluorine doped tin oxide (FTO) substrates.

3.5 Hydrothermal Synthesis of Tungsten trioxide thin films:

A well-known low temperature Hydrothermal Growth method employed for the growth of tungsten trioxide thin films on fluorine doped tin oxide (FTO) substrates.

3.5.1 Substrate cleaning:

The initial step is to clean FTO substrate. We select F-doped SnO_2 (FTO) substrate rather than ITO as conductivity of ITO is ~2 times higher than FTO, but it has poor thermal stability and chemical resistivity [47]. It makes better choice for conducting substrate. Gold and platinum generally used for high-work function back-contacts. [48]. ITO films decreases above 350 ^0Cquickly. But FTO and ITO/FTO coatings mostly stable up to 600– 700 ^0C [49-55].

Firstly, kept the FTO's in acetone for 1 hour and 30 minutes for sonication, then place them in the ethanol for 1 hour followed by sonication. At the end sonicate FTO's for 30 minutes in distilled water. After sonication annealed dry them at 100^{0}C for 30 minutes.

Figure 3.1: Washed FTO's by sonication

3.5.2 Deposition of WO_3 Thin films on FTO:

Following steps were followed for the synthesis of the Tungsten trioxide thin films via Hydrothermal method.

- Firstly, 1.46g of sodium tungstate dihydrate powder ($Na_2WO_4.2H_2O$) was dissolved in 50ml of deionized water.
- Now add HCl (3M) drop wise in prepared solution until light milky translucent stage not reached and the PH of solution reaches 2(acidic).

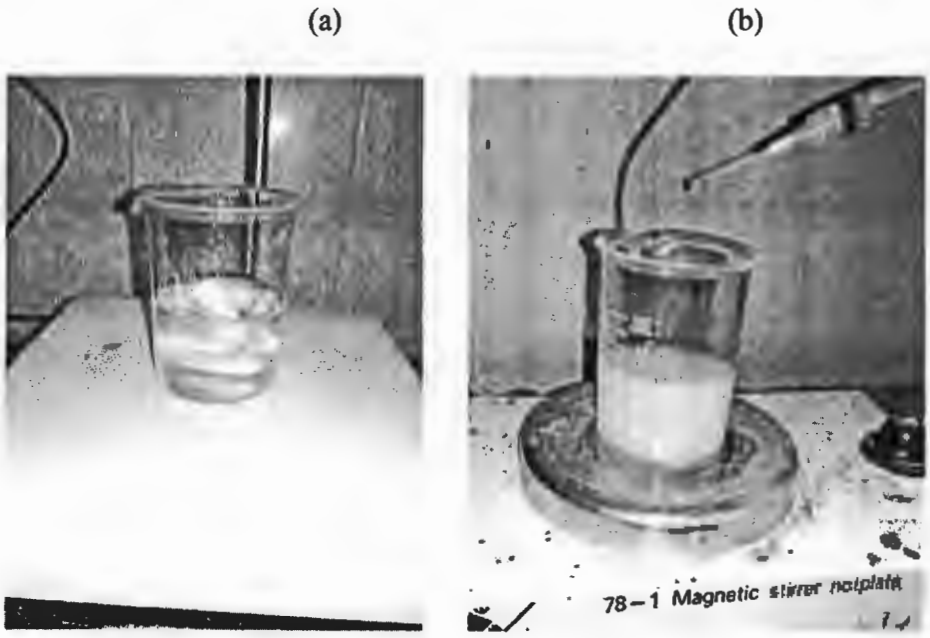

Figure 3.2: (a) solution without HCl, (b) solution added dropwise HCl

- Then Prepared FTO's substrate for growth stage with a back contact with Teflon tape.

Figure 3.3: FTO's Prepared for growth stage.

- After that solution transferred into the autoclave with FTO substrate in such a way that the conducting side facing down. The hydrothermal process was carried out at 140^0 C temperature for 4hours.

Figure 3.4: Substrate fixed into a Teflon holder with face down conducting side.

- After completion of reaction, the samples were removed from solution, rinsed with deionized water 3-4 times, dried at room temperature and then annealed for 2h at 400^0C.

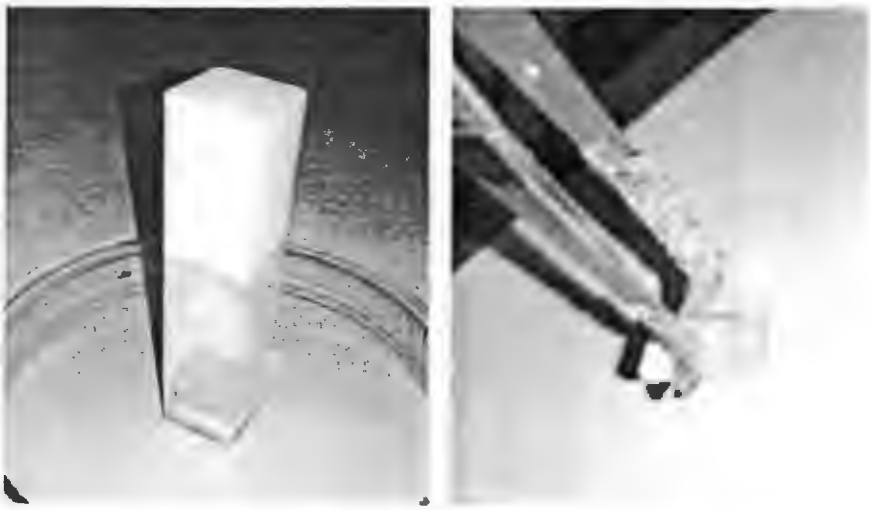

Figure 3.5: Uniform deposition of WO3 thin films on FTO substrate.

3.6 Different ways to obtain graphene oxide sheets:

Different synthesis routes can be followed to prepare the graphene oxide sheets such as:

- Brodie method
- Staud's method
- Fast and facile method
- Hummer's method
- Improved Hummer's method
- Modified Hummer's method

I followed the Modified Hummer's method to synthesized the graphene oxide nanosheets

3.7 Why Modified Hummer's Method?

I followed the modified Hummer's method to synthesized the graphene oxide nanosheets because

- Safe route for the synthesis of GO Nano sheets.
- Achievement of better exfoliation state and faster oxidation rate.
- High productivity of final oxidized product with the decrease demand of acid.

3.8 Synthesis of GO through modified hummers method by using expanded graphite as precursor:

3.8.1 Formation of the Expanded Graphite:

Following steps were followed to form expanded graphite.

- In the mixture of the concentrated solution of the nitric acid (HNO_3) and the sulphuric acid (H_2SO_4) of the same ratio (30ml:30ml), adding 15g of the graphite powder in it and then kept it for three days at the room temperature to expand graphite.
- Because of this process, sulphate ions and nitrate ions were introducing that's become the reason of causing the expansion between the graphite planes.
- The fluffy texture of the final expanded graphite was observed from the expansion of the graphite and consider it be having very low density.

3.8.2 Synthesis of Graphene oxide:

- Initially, 40ml of sulphuric acid (H_2SO_4) is added in a beaker and stirr it for about 10 minutes at room temperature.
- Then 2.5gm of expanded graphite is added in small intervals and kept it on stirring at room temperature.
- The beaker was then placed in an ice bath and 7.5gm of potassium permanganate $KMNO_4$ was added in the beaker with small intervals and kept continuous very slow stirring until a uniform liquid paste was formed.

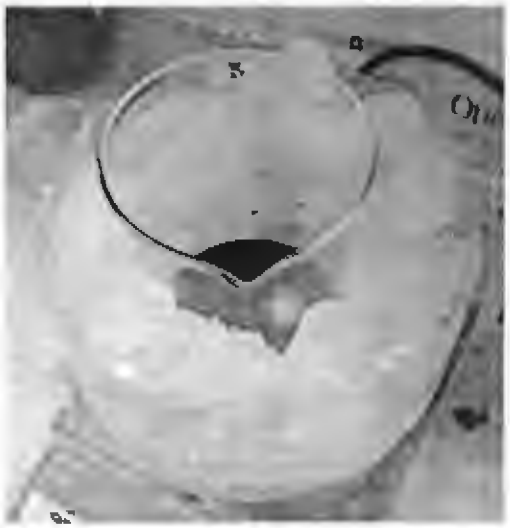

Figure 3.6: Ice bath while adding potassium permanganate

- After the formation of this paste, ice bath was removed and a paste with dark green colour was formed.
- After the dark green colour paste attained, stirring was stopped until a foam like intermediate was formed and large volumetric expansion took place around 30 minute at room temperature.
- Then deionized water was added in the solution for dilution and rapid stirring was carried out until a brown coloured solution was appeared.
- Then solution was placed in a water bath for uniform heating at 90^0C for 2 hours that gave dark green colour to solution again.

Figure 3.7: Heating reactants in water bath

- 2ml H_2O_2 was added in the solution after the removal of water bath and due to this addition yellowish bubbles started to appear.
- Above mentioned solution was centrifuged to separate the particle.
- To remove the impurities of the metal ions 1M solution of HCl was added to the solution and continuously slow stirring was maintained for about 3-4 hours. To separate the particles of graphene oxide solution was centrifuged again.
- Deionized water was added in obtained particles to remove unwanted HCl and kept it on stirring for half an hour and again apply the centrifugation phenomenon.

Figure 3.8: Addition of deionized water

- Also, final washing was carried out by adding deionized water and ethanol to wash out unwanted acid. To get separated particles centrifuged the above solution.

- Appropriate amount of the graphene oxide solution was spread over substrate completely and allowed to stand for 30 s and 60 s and spin coated at 1500 rpm and 3000 rpm respectively.
- After that, the prepared samples were dried for 24 h at room temperature.

CHAPTER NO. 4

4 Results and Discussion

Structural Analysis:

4.1 X-Ray diffraction analysis:

4.1.1 XRD analysis of WO_3 Thin films:

Figure 4.1 represents the x-ray diffraction (XRD) pattern for the determination of crystalline structure of WO_3 thin films. The outcomes demonstrated the mixed phases of tetragonal (α-WO_3) and monoclinic (γ-WO_3) matched with the JCPDS card number (85-0808) and (83-0950). Peaks were observed at 2θ= 23.07°, 25.72°, 26.81°, 31.79°, 33.97°, 42.85°, 51.72° and 54.68° alongside the miller indices (110), (200), (101), (022), (200), (222), (112) and (310) respectively. The sharp and intense diffraction peaks show a high degree of crystallinity of the product. Several peak of FTO's represented at different angles. No additional peaks are found. Such results resembled with the previously reported work by V.V. Kondalkar et al., [56].

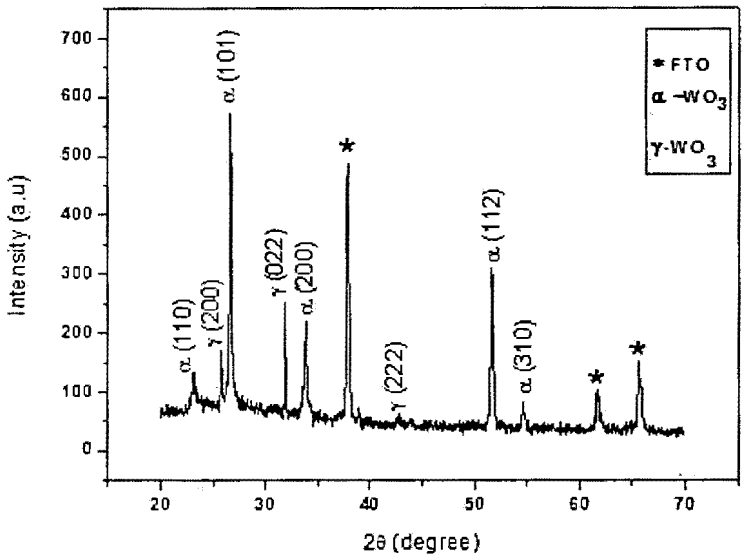

Figure 4.1: XRD pattern of tungsten trioxide(WO_3) Thin film

Calculation of Crystallite size:

Crystallite size was determined by using Debye Scherer equation.

$$D = k\lambda / \beta\cos\theta$$

Where,

D= Crystalline size in nanometre.

K= Constant which is 0.9.

λ = Wavelength of x-rays which is 0.154Å.

β= Full width at half maximum.

θ= Bragg's angle in degree.

The calculated crystalline size from the Debye Scherrer's formula was 40nm.

4.1.2 XRD analysis of modified WO_3 Thin films with GO:

Figure 4.2 represents the x-ray diffraction (XRD) pattern of modified WO_3 thin films with GO. Graphene oxide shows its prominent peak at 2θ=10.21° indicating the (001) plane. Peaks of WO_3 were observed at 2θ=15.96°,25.72°, 26.81°, 31.79°, 33.97°, 42.85° and 51.72° alongside the miller indices (020), (200), (101), (022), (200) and (112) respectively. Several peak of FTO's represented at different angles. No additional peaks are found.

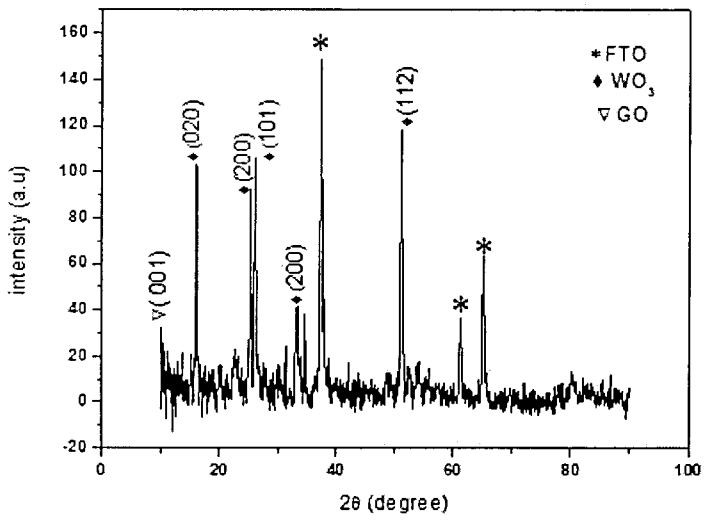

Figure 4.2: XRD pattern of modified tungsten trioxide(WO_3) thin films with GO

Comparative XRD analysis:

Figure 4.3, shows the comparative XRD patterns of pure WO_3 thin films and modified WO_3 thin films with GO. Pure WO_3 thin films shows prominent peak at $2\theta=26.81°$ indicating (101) plane. After modifying WO_3 thin films with GO, the intensity of (101) peak at $2\theta=26.81°$, which is identified as the main peak of the WO_3 phase, gradually decreases. In modified WO_3 thin films no additional peaks are obtained, recommending that no considerable chemical reaction was taken place between WO_3 and GO.

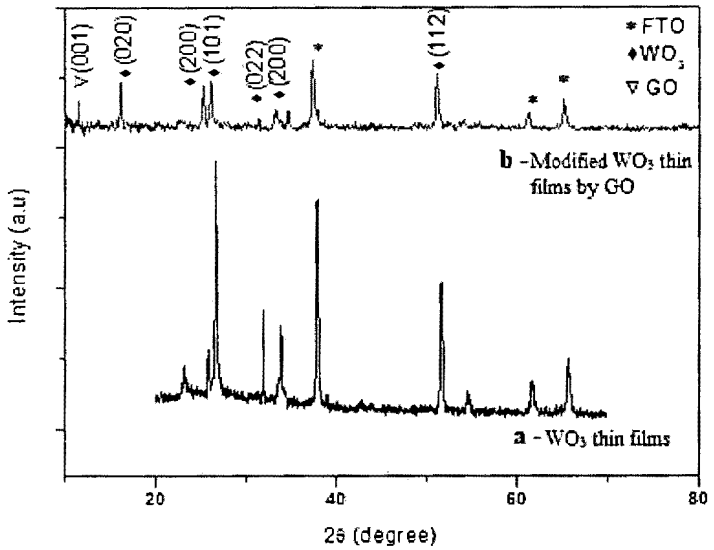

Figure 4.3: Comparative XRD analysis of (a)- WO_3 thin films and (b)- modified WO_3 thin films with GO

Morphological Investigations

4.2 Scanning Electron Microscope Examination:

4.2.1 SEM analysis of WO_3 Thin films:

The morphologies and microstructures of pure WO_3 thin films are revealed by the SEM micrographs. Figures 4.4 shows SEM images of WO_3 thin films which were deposited on fluorine-doped tin oxide (FTO) substrates, by hydrothermal method with nanobrick like morphology, at different magnification i.e 1μm, 2μm, 5μm and 500 nm. Images shows the randomly arranged WO_3 nanobricks. Such results resembled with the previously reported work by V.V. Kondalkar et al.,[56].

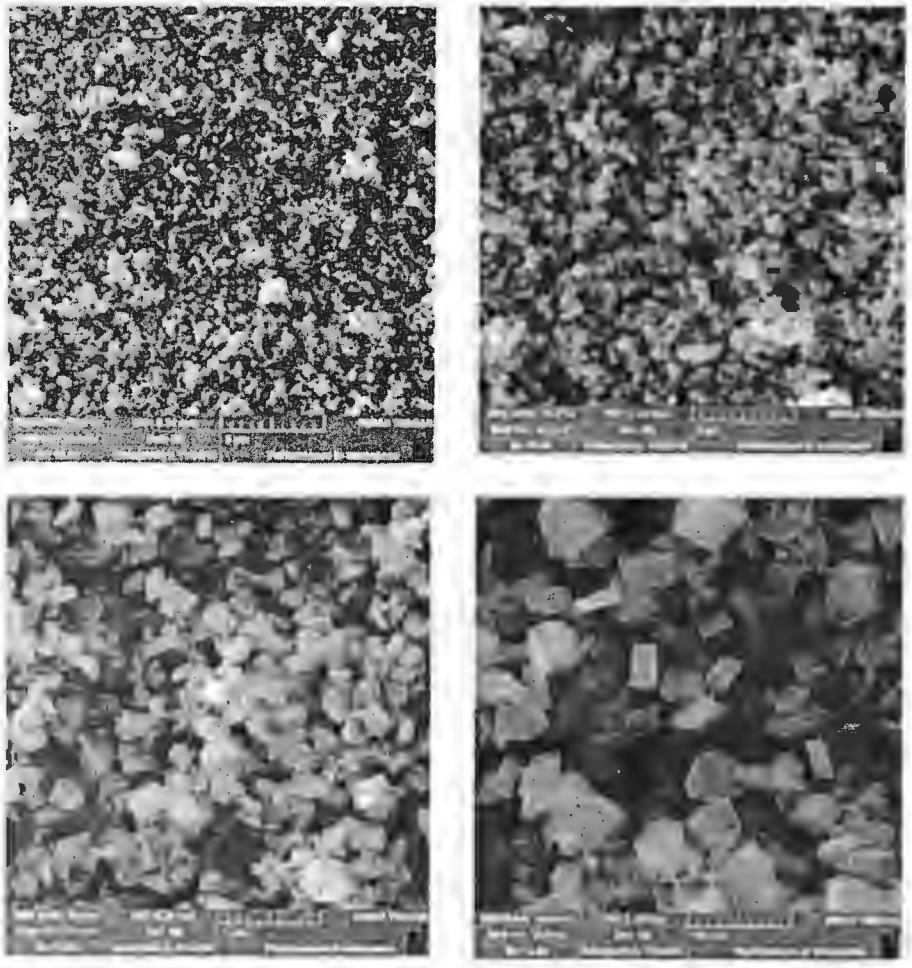

Figure 4.4: SEM analysis of WO_3 thin films at different magnification.

4.2.2 SEM analysis of modified WO_3 thin films with GO:

The morphologies and microstructures of modified WO_3 thin films with GO are revealed by the SEM micrographs. Figures 4.5 shows SEM images of modified WO_3 thin films with GO through spin coating, at different magnification i.e. 50μm, 2μm, 5μm and 10 μm. The SEM results shows that modified WO_3 Nano bricks are folded with GO sheets and it is feasible to differentiate the edges of single nano brick.

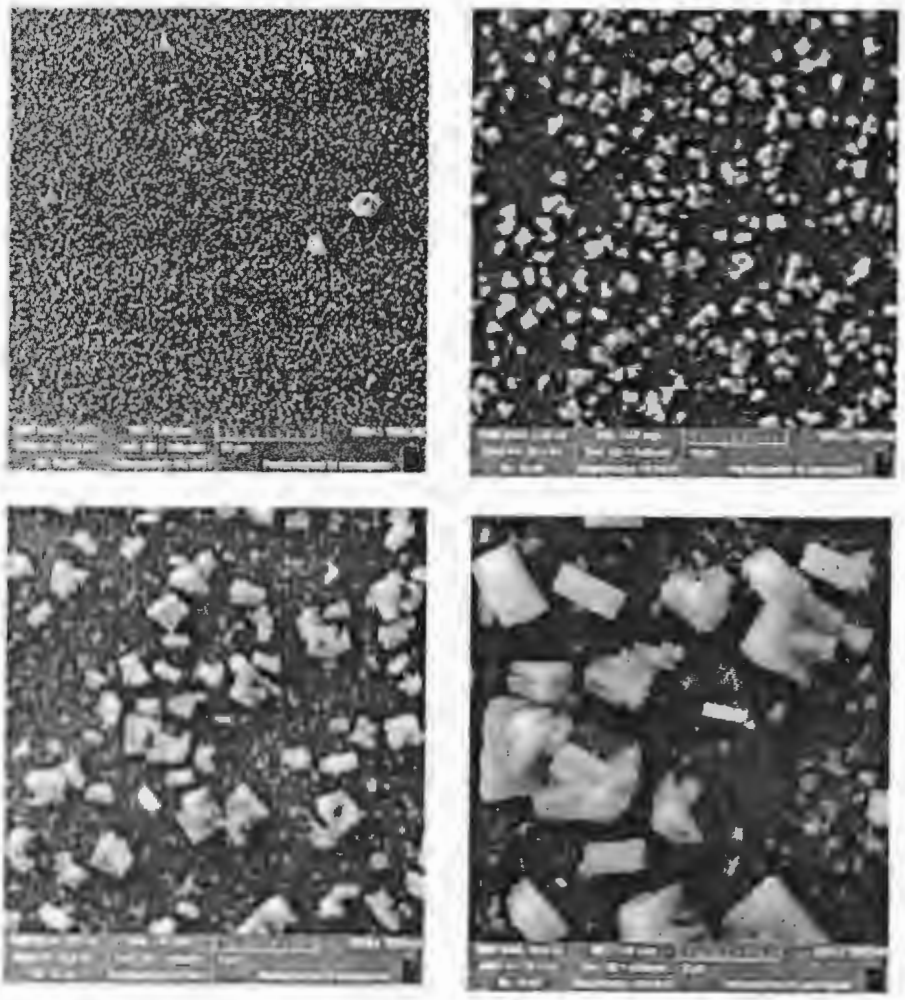

Figure 4.5:SEM analysis of modified WO_3 thin films with GO at different magnifications

Compositional Analysis

4.3 EDX (Energy Dispersive X-ray Analysis)

4.3.1 EDX Analysis of WO_3 Thin films:

EDX analysis is carried out to get the elemental analysis of WO_3 thin films. EDS spectra gives different elemental data in WO_3 thin films, and observed peaks are of Sn, W, Na, O, C, respectively. Sn peak is due to the FTO substrate and it shows that film prepared is very thin and table shows their weight percentage and atomic percentage in WO_3 thin film.

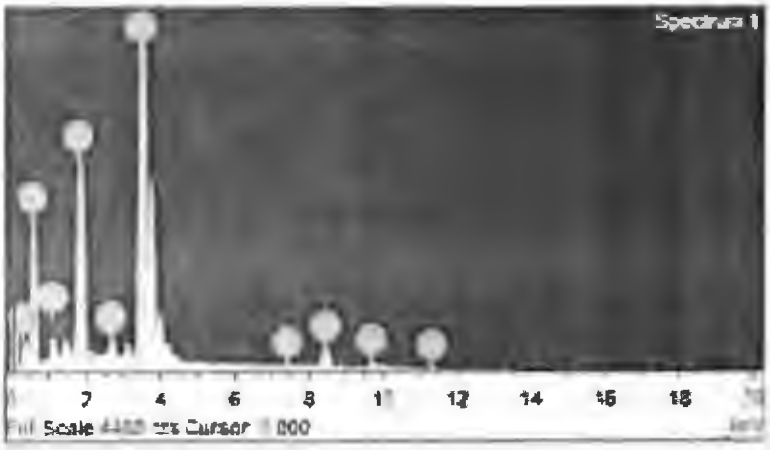

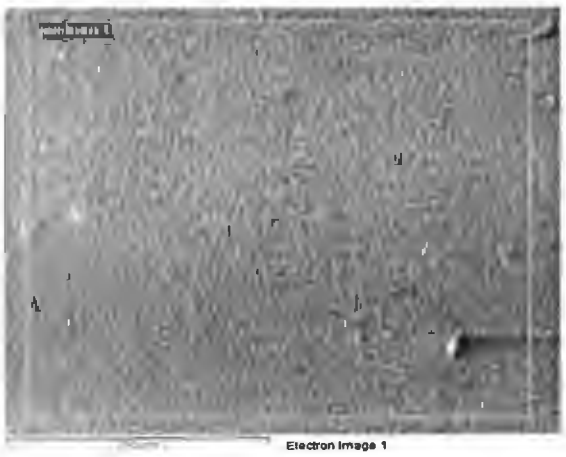

Element	Weight%	Atomic%
C K	3.68	10.79
O K	31.79	69.95
Na K	1.17	1.80
Sn L	44.71	13.26
W M	17.87	3.42
Totals	100.00	

Figure 4.6: EDX spectra of WO_3 thin film, area selected for EDX analysis and weight % present in WO_3 thin film.

4.3.2 EDX analysis of modified WO_3 thin films with GO:

EDX analysis is carried out to get the elemental analysis of modified WO_3 thin films with GO. EDX spectra gives different elemental data in modified WO_3 thin films with GO, and observed peaks are of Sn, W, O, C, respectively. Sn peak is due to the FTO substrate and it shows that film prepared is very thin and table shows their weight percentage and atomic percentage in WO_3 thin film.

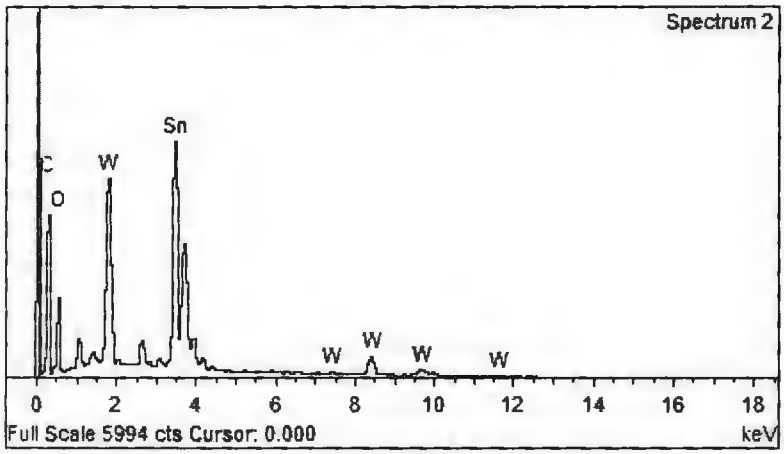

Element	Weight %	Atomic %
C K	23.45	52.81
O K	21.35	36.11
Sn L	36.57	8.34
W M	18.63	2.74
Totals	100.00	

Figure 4.7: EDX spectra of modified WO_3 thin film by GO, area selected for EDX analysis and weight % present in modified WO_3 thin film by GO.

Optical Analysis:

4.4 UV-Vis spectroscopy analysis:

4.4.1 UV-Vis analysis of WO_3 thin film:

Figure 4.8 shows the UV-Visible analysis of WO_3 thin film prepared hydrothermally. Maximum peak is observed at a wavelength of 523nm, which is in visible range. The band gap energy (E_g) is calculated on the basis of the maximum absorption band of WO_3 thin films and is obtained to be 2.37eV according to following equation.

$$Eg = 1239.8/\lambda max$$

Light is absorbed in the wavelength range of 400-750nm.

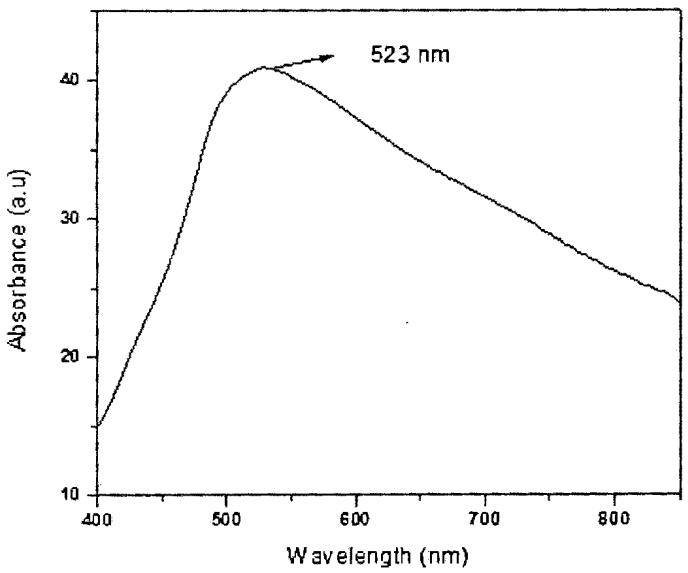

Figure 4.8: UV-Vis analysis of WO_3 thin films

4.4.2 UV-Vis analysis of modified WO_3 thin film by GO:

Figure 4.9 shows the UV-Visible analysis of WO_3 thin film which are modified with GO through spin coating. Maximum peak is observed at a wavelength of 498nm, which is in visible range. The band gap energy (E_g) is calculated on the bsasis of the maximum absorption band of modified WO_3 thin films with GO and is obtained to be 2.48 eV. The additional broad absorption was exhibited by modified WO_3 thin films in the visible region which lies in the range of 700-800 nm. This absorption is due to O^{2-}–W^{6+} charge transfer transition, as in case of monoclinic WO_3. Light is absorbed in the wavelength range of 450-800nm.

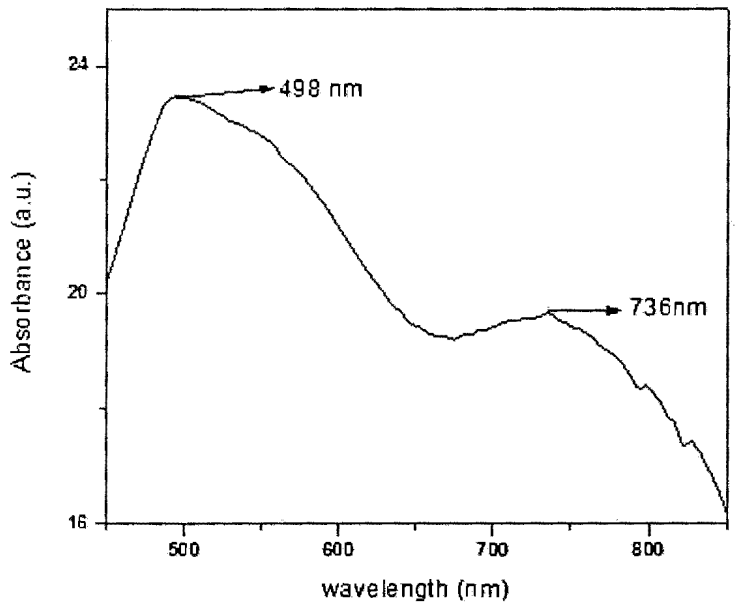

Figure 4.9: UV-Vis analysis of modified WO_3 thin films with GO.

Conclusions:

Tungsten trioxide (WO_3) thin films are synthesized by hydrothermal method and Graphene Oxide has been successfully synthesized by utilizing the modified hummer's method. Modification of Tungsten trioxide (WO_3) thin films with Graphene Oxide is done through the spin coating method. The calculated crystalline size for pure WO_3 is 40 nm. SEM study showed that WO_3 thin films has a brick like morphology while modified WO_3 Nano bricks are coated by GO sheets, it is feasible to differentiate the edges of single Nano brick. Chemical composition of each sample was determined by using EDX and results shows the purity of synthesized films. UV-vis spectroscopy shows that Maximum absorption of WO_3 is found at a wavelength of 523 nm while for modified WO_3 with GO Maximum absorption is found at 498 nm.

References

1. Guillen, C. and J. Herrero, High conductivity and transparent ZnO: Al films prepared at low temperature by DC and MF magnetron sputtering. Thin Solid Films, 2006. **515**(2): p. 640-643.
2. Poortmans, J. and V. Arkhipov, Thin film solar cells: fabrication, characterization and applications. Vol. 5. 2006: John Wiley & Sons.
3. Cachet, H., Cortes, R., Froment, M., & Etcheberry, A. (2000). Electrodeposition of epitaxial CdSe on (111) gallium arsenide. Thin Solid Films, 2000. **361**: p. 84-87.
4. Patidar, D., Rathore, K. S., Saxena, N. S., Sharma, K., & Sharma, T. P. (2008). Energy band gap and conductivity measurement of CdSe thin films. Chalcogenide Letters, 2008. **5**(2): p. 21-25.
5. Eckertova, L., Physics of thin films. 2012: Springer Science & Business Media.
6. Niesen, T.P. and M.R. De Guire, Review: deposition of ceramic thin films at low temperatures from aqueous solutions. Journal of Electroceramics, 2001. **6**(3): p. 169-207.
7. Bunshah, R.F., Handbook of hard coatings. 2001.
8. Sharma, M., Kumar, S., Sharma, L. M., Sharma, T. P., & Husain, M. (2004). Characterization of CdSe x Te 1− x sintered films. Current Applied Physics, 2004. **4**(5): p. 419-425.
9. Lockhart, M., Clabon, L., Lott, C., James, M., Ali, W. H., & Northern, J. (2008, April). Automated battery tester data acquisition system using labview. in Region 5 Conference, 2008 IEEE. 2008. IEEE.
10. Deb, S.K., Opportunities and challenges in science and technology of WO_3 for electrochromic and related applications. Solar Energy Materials and Solar Cells, 2008. **92**(2): p. 245-258.
11. Weil, M. and W.-D. Schubert, The Beautiful Colours of Tungsten Oxides. Newsletter, 2013.
12. Zheng, H., Ou, J. Z., Strano, M. S., Kaner, R. B., Mitchell, A., & Kalantar-zadeh, K. (2011). Nanostructured tungsten oxide–properties, synthesis, and applications. Advanced Functional Materials, 2011. **21**(12): p. 2175-2196.
13. Gerand, B., Nowogrocki, G., Guenot, J., & Figlarz, M. (1979). Structural study of a new hexagonal form of tungsten trioxide. Journal of Solid State Chemistry, 1979. **29**(3): p. 429-434.

14. Liu, X., F. Wang, and Q. Wang, Nanostructure-based WO_3 photoanodes for photoelectrochemical water splitting. Physical Chemistry Chemical Physics, 2012. **14**(22): p. 7894-7911.

15. Guo, Y., Murata, N., Ono, K., & Okazaki, T. (2005). Production of ultrafine particles of high-temperature tetragonal WO_3 by dc arc discharge in Ar–O 2 gases. Journal of Nanoparticle Research, 2005. **7**(1): p. 101-106.

16. Vijayalakshmi, R., Jayachandran, M., Trivedi, D. C., & Sanjeeviraja, C. (2006). Characterization of WO_3 thin films prepared at different deposition currents on CTO substrates. Synthesis and Reactivity in Inorganic, Metal-Organic and Nano-Metal Chemistry, 2006. **36**(1): p. 89-94.

17. Ng, C., Ye, C., Ng, Y. H., & Amal, R. (2010). Flower-shaped tungsten oxide with inorganic fullerene-like structure: synthesis and characterization. Crystal Growth & Design, 2010. **10**(8): p. 3794-3801.

18. Berger, S., Tsuchiya, H., Ghicov, A., & Schmuki, P. (2006). High photocurrent conversion efficiency in self-organized porous WO_3. Applied Physics Letters, 2006. **88**(20): p. 203119.

19. Huang, J. and Q. Wan, Gas sensors based on semiconducting metal oxide one-dimensional nanostructures. Sensors, 2009. **9**(12): p. 9903-9924.

20. Zheng, J.Y., Haider, Z., Van, T. K., Pawar, A. U., Kang, M. J., Kim, C. W., & Kang, Y. S. (2015).Tuning of the crystal engineering and photoelectrochemical properties of crystalline tungsten oxide for optoelectronic device applications. CrystEngComm, 2015. **17**(32): p. 6070-6093.

21. Patnaik, P., Handbook of inorganic chemicals. Vol. 529. 2003: McGraw-Hill New York.

22. Zhao, J., L. Liu, and F. Li, Graphene oxide: physics and applications. 2015: Springer.

23. Boukhvalov, D.W. and M.I. Katsnelson, Modeling of graphite oxide. Journal of the American Chemical Society, 2008. **130**(32): p. 10697-10701.

24. Lahaye, R., J. W. E., Jeong, H. K., Park, C. Y., & Lee, Y. H. (2009). Density functional theory study of graphite oxide for different oxidation levels. Physical Review B, 2009. **79**(12): p. 125435.

25. Eda, G., G. Fanchini, and M. Chhowalla, Large-area ultrathin films of reduced graphene oxide as a transparent and flexible electronic material. Nature nanotechnology, 2008. **3**(5): p. 270-274.

26. Hofmann, U. and R. Holst, The acidic nature and the methylation of graphitoxide. Berichte der deutschen chemischen Gesellschaft, 1939. **72**: p. 754-771.
27. Ruess, G., Über das graphitoxyhydroxyd (graphitoxyd). Monatshefte für Chemie und verwandte Teile anderer Wissenschaften, 1947. **76**(3-5): p. 381-417.
28. Scholz, W. and H. Boehm, Untersuchungen am graphitoxid. VI. Betrachtungen zur struktur des graphitoxids. Zeitschrift für anorganische und allgemeine Chemie, 1969. **369**(3-6): p. 327-340.
29. Dreyer, D.R., et al., The chemistry of graphene oxide. Chemical Society Reviews, 2010. **39**(1): p. 228-240.
30. Hummers Jr, W.S. and R.E. Offeman, Preparation of graphitic oxide. Journal of the American Chemical Society, 1958. **80**(6): p. 1339-1339.
31. Jiao, Z., et al., Morphology-tailored synthesis of tungsten trioxide (hydrate) thin films and their photocatalytic properties. ACS applied materials & interfaces, 2011. **3**(2): p. 229-236.
32. Huang, K., et al., Controllable synthesis of hexagonal WO3 nanostructures and their application in lithium batteries. Journal of Physics D: Applied Physics, 2008. **41**(15): p. 155417.
33. Chan, S.H.S., et al., Recent developments of metal oxide semiconductors as photocatalysts in advanced oxidation processes (AOPs) for treatment of dye waste-water. Journal of Chemical Technology and Biotechnology, 2011. **86**(9): p. 1130-1158.
34. Zhao, Y., et al., One-pot twelve tungsten phosphate acid assisted electrochemical synthesis of WO_3-decorated graphene sheets for high-efficiency UV-light-driven photocatalysis. Chemical Physics Letters, 2014. **607**: p. 34-38.
35. Penza, M., C. Martucci, and G. Cassano, NO x gas sensing characteristics of WO 3 thin films activated by noble metals (Pd, Pt, Au) layers. Sensors and Actuators B: Chemical, 1998. **50**(1): p. 52-59.
36. Huo, N., et al., Synthesis of WO_3 nanostructures and their ultraviolet photoresponse properties. Journal of Materials Chemistry C, 2013. **1**(25): p. 3999-4007.
37. Acosta, M., D. González, and I. Riech, Optical properties of tungsten oxide thin films by non-reactive sputtering. Thin Solid Films, 2009. **517**(18): p. 5442-5445.
38. Wang, Z.-g., et al., The green synthesis of reduced graphene oxide by the ethanol-thermal reaction and its electrical properties. Materials Letters, 2014. **116**: p. 416-419.

39. Jie, X., et al., Graphene-wrapped WO 3 nanospheres with room-temperature NO 2 sensing induced by interface charge transfer. Sensors and Actuators B: Chemical, 2015. **220**: p. 201-209.

40. Song, J., X. Wang, and C.-T. Chang, Preparation and Characterization of Graphene Oxide. Journal of Nanomaterials, 2014. **2014**.

41. An, X., et al., WO_3 nanorods/graphene nanocomposites for high-efficiency visible-light-driven photocatalysis and NO_2 gas sensing. Journal of Materials Chemistry, 2012. **22**(17): p. 8525-8531.

42. Choobtashani, M. and O. Akhavan, Visible light-induced photocatalytic reduction of graphene oxide by tungsten oxide thin films. Applied Surface Science, 2013. **276**: p. 628-634.

43. Thangavel, S., M. Elayaperumal, and G. Venugopal, Synthesis and properties of tungsten oxide and reduced graphene oxide nanocomposites. Materials Express, 2012. **2**(4): p. 327-334.

44. Luévano-Hipólito, E., et al., Precipitation synthesis of WO 3 for NO x removal using PEG as template. Ceramics International, 2014. **40**(8): p. 12123-12128.

45. Zhang, J., et al., Electrochromic behavior of WO 3 nanotree films prepared by hydrothermal oxidation. Solar Energy Materials and Solar Cells, 2011. **95**(8): p. 2107-2112.

46. Livage, J. and D. Ganguli, Sol–gel electrochromic coatings and devices: a review. Solar Energy Materials and Solar Cells, 2001. **68**(3): p. 365-381.

47. Gordon, R.G., Criteria for choosing transparent conductors. MRS bulletin, 2000. **25**(08): p. 52-57.

48. Cui, Y. and C.M. Lieber, Functional nanoscale electronic devices assembled using silicon nanowire building blocks. science, 2001. **291**(5505): p. 851-853.

49. Minami, T., New n-type transparent conducting oxides. Mrs Bulletin, 2000. **25**(08): p. 38-44.

50. Sullivan, I., et al., Cu-Deficiency in the p-Type Semiconductor Cu5–x Ta11O30: Impact on Its Crystalline Structure, Surfaces, and Photoelectrochemical Properties. Chemistry of Materials, 2014. **26**(23): p. 6711-6721.

51. Ferekides, C., et al., Transparent conductors and buffer layers for CdTe solar cells. Thin Solid Films, 2005. **480**: p. 224-229.

52. Fortunato, E., et al., Transparent conducting oxides for photovoltaics. MRS bulletin, 2007. **32**(03): p. 242-247.

53. Minami, T., T. Miyata, and T. Yamamoto, Stability of transparent conducting oxide films for use at high temperatures. Journal of Vacuum Science & Technology A: Vacuum, Surfaces, and Films, 1999. **17**(4): p. 1822-1826.

54. Abe, R., M. Higashi, and K. Domen, Facile fabrication of an efficient oxynitride TaON photoanode for overall water splitting into H2 and O2 under visible light irradiation. Journal of the American Chemical Society, 2010. **132**(34): p. 11828-11829.

55. Goto, K., T. Kawashima, and N. Tanabe, Heat-resisting TCO films for PV cells. Solar energy materials and solar cells, 2006. **90**(18): p. 3251-3260.

56. Kondalkar, V., et al., Nanobrick-like WO 3 thin films: hydrothermal synthesis and electrochromic application. Superlattices and Microstructures, 2014. **73**: p. 290-295.